Journal of Solid State Chemistry **150,** 286–293 (2000)
doi:10.1006/jssc.1999.8593, available online at http://www.idealibrary.com on IDEAL®

The Structure and Properties of Graphite Monofluoride Using the Three-Dimensional Cyclic Cluster Approach

A. Zajac,*,§,[1] P. Pelikán,†,§,‖ J. Minár,† J. Noga,‡,§ M. Straka,‖,¶ P. Baňacký,*,§ and S. Biskupič†,§

*Institute of Chemistry, Faculty of Natural Sciences, Comenius University, SK-84215 Bratislava, Slovakia; †Department of Physical Chemistry, Slovak University of Technology, SK-81237 Bratislava, Slovakia; ‡Institute of Inorganic Chemistry, Slovak Academy of Sciences, SK-84236 Bratislava, Slovakia; §S-Tech, Inc., Uršulínska 3, SK-81101 Bratislava, Slovakia; ‖Faculty of Chemistry, Technical University Brno, CZ-63700 Brno, Czech Republic; and ¶Department of Chemistry, University of Helsinki, P.O. Box 55, FIN-00014, Finland

Received August 11, 1999; in revised form November 15, 1999; accepted December 4, 1999

In this paper, we present the theoretical study of the crystal and electron structure of an intercalated compound of graphite —the graphite monofluoride $\{CF\}_n$. The latter is widely used as a lubricant under extremely high temperatures and high vacuum, and as a successful cathodic depolarizer in batteries with high energy density. The layered structure of the graphite monofluoride has been confirmed, but statistical distributions of the individual layers are possible. This fact helps in understanding the problems linked to an experimental determination of the structure of this material. Small interlayer dissociation energies show that the bonding between the individual layers is mainly due to the weak interlayer electrostatic forces, which explains the excellent lubricant properties of this material. Band structure calculations reveal that, whereas some layer arrangements of the bulk material lead to insulating properties, others have a conductive character. This fact explains the weak overall conductive properties of synthetic graphite monofluoride.

Key Words: **intercalated graphite; graphite monofluoride; geometric structure; band structure; electric conductivity.**

INTRODUCTION

Even though the discovery of intercalation of graphite dates to the 1940s (1–4), and the properties of the corresponding synthetic compounds and explanation of the underlying reactions have been studied for few decades later, there are, yet, several questions to be answered. Intercalated compounds of graphite are formed by the penetration of atoms within the lamellar structure of graphite without destruction of the host's layered bonding network (5). The graphite sheets may be viewed as huge aromatic macromolecules bonded together by weak intermolecular bonds. The bonding between carbon atoms in the infinite six-member aromatic sheets involves σ-sp^2 hybridized orbitals (6). The remaining electrons (one per carbon) enter the delocalized orbitals of the π-p_z symmetry, which causes an aromatic character of the sheets and, in addition, these electrons share the bonding between the odd sheets. These π-electrons can give rise to bonds with fluorine atoms upon intercalation. Formation of these bonds may lead to changes of the bonding character of original graphite, its electron structure, and its properties.

Fluorination of graphite leads (1, 2, 4, 7–9) to the formation of a series of materials composed of $\{CF_x\}_n$ units ($x = 0.2$–1.2), sometimes referred to as "graphite fluorides." The ionic or semi-ionic $\{CF_x\}_n$ are prepared at an ambient temperature in the presence of an acidic fluoride such as HF. The electrical conductivity is increased by one order of magnitude at the early stage of intercalation, and then it is substantially decreased with a progress in the fluorine intercalation. Based on its conductivity properties, the two aforementioned types of graphite fluorides are divided into two different groups: those with covalent bonds and those with ionic bonds. Within the huge variety of the graphite fluorides the stoichiometric compounds $\{CF\}_n$, $\{C_2F\}_n$, and $\{C_4F\}_n$ are of special interest. The most stable is $\{CF\}_n$, i.e., the "graphite monofluoride." Graphite monofluoride is an excellent lubricant under extremely high temperatures and high vacuum (10–13), and it is also a quite successful cathodic depolarizer in batteries with high energy density (14–17).

Structure of the layered graphite monofluoride is derived from graphite by insertion of covalently bonded fluorine atoms above and below each hexagon in each layer (9, 10, 18–20). By forming these C–F covalent bonds with the carbon atoms, fluorine atoms disrupt the aromatic network and form a carbon skeleton in which each carbon is bound by four covalent bonds with nonequivalent sp^3 hybridization. The destruction of the π-aromatic carbon skeleton generates only slightly conducting (21) graphite derivatives in which single carbon sheets are buckled rather than planar.

[1] To whom correspondence should be addressed.

0022-4596/00 $35.00

The determination of the structure of graphite monofluoride is connected with great problems (9), due to difficulties in growing a single crystal of a sufficient size. Without doubt, the carbon layers in graphite monofluoride are puckered. The Rüdorff's structure (3, 4) assumed an infinite array of *trans*-linked cyclohexane chairs. An infinite array of *cis-trans*-linked cyclohexane boats is another possible conformation. Based on X-ray powder diffraction studies (9, 22, 23), the chair structure in a hexagonal crystal lattice ($P6_3mc$ symmetry group) was predicted. In contrast, studies of NMR second moment measurements (24, 25) indicate a boat structure, which results in an orthorhombic crystal lattice (*Pmm*2 symmetry group). Both these conformations correspond to approximately tetrahedral coordinated sp^3 hybridized carbon atoms.

In the case of chair conformation of the graphite monofluoride, various types of the arrangement of individual layers are possible. In view of the aforementioned facts, even the determination of the mutual arrangements of individual layers using X-ray diffraction data is an overwhelming problem. The aim of the present paper is to contribute in clarifying some of the above-mentioned problems connected with the structure and properties of graphite monofluoride using theoretical considerations and numerical calculations. To the best of our knowledge, there was only one theoretical study of the graphite monofluoride published in the past (6), leaving some of the problems outlined above open for further discussion.

METHOD OF CALCULATION

The Cluster Crystal Orbital (26, 27) method, presented in our previous papers, was applied in all our calculations. Within this method, extremely large finite clusters containing tens of thousands of atoms are considered. This leads to inclusion of the long-range interactions, which, in general, have an important influence on the electron properties of a solid state system. In this method, the modulo-periodic boundary conditions ensure the periodicity of the wave functions, eliminate the so-called boundary effects (the fact that bonds on the boundaries of a given cluster are unsaturated), and allow the use of transformation to Bloch orbital basis. Calculation of the electron density based on several thousands points of the first Brillouin zone gives the values of the density matrix close to its bulk limit values. These are further used for band structure calculations.

Finite cluster is built-up by translational replication of the elementary unit cell along the respective lattice vector directions $\mathbf{a}_i (i = 1, 2, 3)$ N_i times. Then, $N = N_1N_2N_3$ is the total number of unit cells considered in the cluster. The idea behind the cyclic cluster approach is to impose the same surroundings to all unit cells of the cluster. The interactions of the central unit cell are imposed on the rest of the cells. By virtue of this, each unit cell of the cluster "feels" such an environment as if it was in the center of the cluster. For a finite cluster of size N, adopting the following identity imposes a "ring periodicity"

$$\mathbf{R} + \mathbf{R}' = \sum_{i=1}^{3} \left\{ n_i + n_i' - N_i . \mathrm{int}\left(\frac{2(n + n_i')}{N_i} \right) \right\} \mathbf{a}_i . \quad [1]$$

For a cluster constructed in this way, the translation symmetry is guaranteed, and for any one-particle ($\hat{h}$) and two-particle ($\hat{g}$) operator the translation periodicity (Born–Karman periodic conditions) within the considered cluster

$$\langle p^{\mathbf{R}+\mathbf{R}'} | \hat{h} | q^{\mathbf{R}'} \rangle = \langle p^{\mathbf{R}} | \hat{h} | q^{\mathbf{O}} \rangle = h_{pq}^{\mathbf{RO}} \quad [2]$$

$$\langle p^{\mathbf{R}_1+\mathbf{R}'} q^{\mathbf{R}_2+\mathbf{R}'} | \hat{g} | r^{\mathbf{R}'} s^{\mathbf{R}_3+\mathbf{R}'} \rangle = \langle p^{\mathbf{R}_1} q^{\mathbf{R}_2} | \hat{g} | r^{\mathbf{O}} s^{\mathbf{R}_3} \rangle \quad [3]$$

must be fulfilled for all lattice translations $\mathbf{R}$. Due to the partial ZDO (zero differential overlap) approximation in the INDO method (28), the requirements of Eqs. [2] and [3] are automatically fulfilled for all necessary integrals. Therefore, the transformation to a Bloch orbital basis is ambiguously given by the finite summation

$$F_{pq}^{\mathbf{k}\mathbf{k}'} = F_{pq}^{\mathbf{k}\mathbf{k}} \delta_{\mathbf{k}\mathbf{k}'} = \sum_{\mathbf{R}}^{N} F_{pq}^{\mathbf{k}\mathbf{k}} \exp(i\mathbf{k}.\mathbf{R}), \quad [4]$$

and, consequently, the Fock matrix is factorized into N blocks of the size $M \times M$, with M being the number of atomic orbitals in the elementary unit cell. The cluster choice determines exactly all the $N_{\mathbf{k}} = (N_1N_2N_3 + 1)/2$ independent values of the wave vector $\mathbf{k}$. As demonstrated by our results, the procedures described above result in rapid convergence to the infinite bulk limit. In our calculations, we used the QR-INDO/1 (quasi-relativistic intermediate neglect of differential overlap) method (29, 30), explicitly considering only the valence electrons of atoms. The matrix elements of the Hartree–Fock operator in this treatment are defined as

$$F_{pq}^{\mathbf{RO}} = h_{pq}^{\mathbf{RO}} + \sum_{\substack{\mathbf{R}_1,\mathbf{R}_2 \\ (\mathbf{R}_3 = \mathbf{R}_1 - \mathbf{R}_2)}}^{N} \sum_{r,s}^{\mathrm{cell}} P_{rs}^{\mathbf{R}_3\mathbf{O}} (2\langle p^{\mathbf{R}} r^{\mathbf{R}_1} | \hat{g} | q^{\mathbf{O}} s^{\mathbf{R}_2} \rangle - \langle p^{\mathbf{R}} r^{\mathbf{R}_1} | \hat{g} | q^{\mathbf{R}_2} s^{\mathbf{O}} \rangle) \quad [5]$$

$$P_{pq}^{\mathbf{RO}} = \frac{1}{N} \sum_{\mathbf{k}}^{N} P_{pq}^{\mathbf{k}} \exp(i\mathbf{k}.\mathbf{R}) \quad [6]$$

$$P_{pq}^{\mathbf{k}} = \sum_{m}^{\mathrm{occ}} (c_{pm}^{\mathbf{k}})^* c_{qm}^{\mathbf{k}}, \quad [7]$$

where $P_{pq}^{\mathbf{RO}}$ and $P_{pq}^{\mathbf{k}}$ are elements of the density matrix. With increasing N, the bulk limit can be reached. This limit can, as shown in our recent study (26) be accomplished in

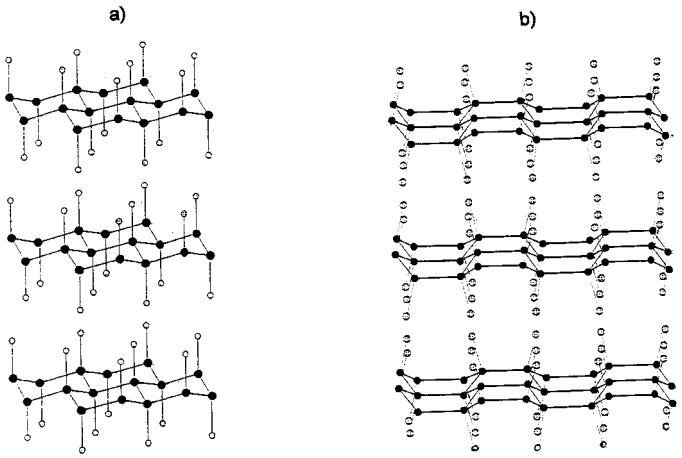

FIG. 1. Two possible conformations of graphite monofluoride: (a) the chair conformation—hexagonal unit cell (symmetry group $P6_3mc$). (b) the boat conformation—orthorhombic unit cell (symmetry group $Pmm2$).

a rather short time. Since for the converged results the density matrix can be treated as one corresponding to the bulk, *a posteriori* calculations for characteristic paths within the first Brillouin zone are fully justified.

The above-mentioned method with QR-INDO/1 Hamiltonian (29, 30) has been implemented within the computer code SOLID98 (33), which has been applied in all calculations presented in this paper.

RESULTS AND DISCUSSION

a. Structures

The main task in this study was (i) to determine which of the possible single-layer conformations (*trans*-cyclohexane chairs or *cis-trans*-linked cyclohexane boats) (see Fig. 1) is more stable and (ii) to determine how these layers can be mutually arranged.

While for the boat conformation one can suggest only a single relevant layer sequence (i.e., fully covered), for the chair conformation there exists several proposals by the crystallographers:

(a) covered configuration with AAA type of sequences;

(b) the configuration in which each second layer is shifted, i.e., *ABAB* type of sequences;

(c) the configuration in which three neighboring layers are mutually shifted, i.e., *ABCABC* type of sequences;

(d) the covered configuration with mirror plane of symmetry, i.e., $AA'/A'A$ type of sequences;

(e) the configuration with mirror plane of symmetry and with each second layer mutually shifted, i.e., $AB/B'A'$ type of sequences.

Simultaneous optimization of 4 to 7 geometric parameters (see Table 1) was necessary for each sequence. Calculations were performed for about 100 points around the minima for all geometry arrangements. The general form of quadratic energy hypersurface was used, and optimization was performed by means of the nonlinear simulated annealing method (31, 32) followed by the conjugate gradient optimization method (31). The results of optimization are summarized in Tables 1 and 2.

Comparison of the chair and boat structures (Table 1) in the covered (*AAA*) configurations shows that the chair structure is more stable (by about 1 eV) (Table 2), which is in good agreement with recent DFT results for the covered structure (6). In addition, symmetry analysis shows that the transition between the two conformations is a symmetry forbidden reaction. Other stacking sequences (b–e) were not studied in (6).

Since, as mentioned in the Introduction, for the (apparently definitely more stable) chair conformation various geometric arrangements of the layers are possible (i.e., a–e), we decided to investigate all of them. Complete geometries are collected in Table 1. As follows from Table 2 the energies of all configurations are very close (within about 0.5 eV). Despite the fact that the *ABCABC* and $AA'/A'A$ are the most stable, it may be concluded that, in the real structure of graphite monofluoride, a statistical distribution of various types of stacking sequences is feasible. In such arrangements the maximal entropy contribution leads to the minimum Gibbs energy of the system. This behavior is similar to that in graphite, where three types of statistically distributed sequences (*AAA*, *ABAB*, and *ABCABC*) have been found. Since the graphite monofluoride is usually prepared by a straightforward fluorination of graphite, statistical distributions of various stacking sequences may result. The statistical distribution of various stacking sequences helps to understand the problems linked to the experimental determination of the structure of graphite monofluoride.

b. Dissociation Energies

To explain the very interesting lubricant properties of the graphite monofluoride, the interlayer dissociation curves were calculated (see Fig. 2). Results of the calculations show that individual layers are mutually bonded by the weak electrostatic forces only (the dissociation energies does not exceed 0.5 eV), which explains the excellent lubricant properties of these types of solid state materials. Crystal orbital overlap populations confirmed the small interlayer bond energies.

c. Electronic Structure and Conductivity

The results of calculations show that optimized C–F bonds in graphite monofluoride are strong covalent bonds: the C–F distances are in the $1.41–1.45 \times 10^{-10}$ m range for various stacking sequences. The net charges on the carbon atoms ($q = 0.11 \rightarrow 0.14$) and fluorine atoms ($q = -0.11 \rightarrow$

TABLE 1
Optimized Coordinates and Lattice Parameters for Various Stacking Sequences of Graphite Monofluoride (Values Are in 10^{-10} m)

Sequence	Atom	Cartesian coordinates			Lattice parameters
		x	y	z	
AAA	C_1	$(1/\sqrt{3})a$	0	$-$ zc	$a = 2.536$; $c = 4.481$;
(hexagonal)	C_2	$(1/2\sqrt{3})a$	$-a/2$	$+zc$	$z = 0.0516$; $u = 0.3735$;
	F_1	$(1/\sqrt{3})a$	0	$-uc$	
	F_2	$(1\sqrt{3})a$	$-a/2$	$+uc$	
AAA	C_1	ax	$1/2b$	$+zc$	$a = 4.369$; $b = 2.5146$;
(orthorhombic)	C_2	$(1/2 - x)a$	0	$-zc$	$c = 4.586$; $z = 0.06612$;
	C_3	$(1/2 + x)a$	0	$-zc$	$u = 0.3687$; $x = 0.1760$;
	C_4	$-xa$	$1/2b$	$+zc$	$w = 0.02961$;
	F_1	$(-1/4 - w)a$	$1/2b$	$+uc$	
	F_2	$(1/4 + w)a$	0	$-uc$	
	F_3	$(3/4 - w)a$	0	$-uc$	
	F_4	$(3/4 + w)a$	$1/2b$	$+uc$	
ABAB	C_1	0	0	$-zc$	$a = 2.5331$; $c = 8.870$;
(hexagonal)	C_2	$(1/\sqrt{3})a$	0	$+zc$	$z = 0.02580$; $u = 0.1880$;
	C_3	$(1/\sqrt{3})a$	0	$(1/2 + z)c$	
	C_4	$(1/2\sqrt{3})a$	$-1/2a$	$(1/2 - z)c$	
	F_1	0	0	$-uc$	
	F_2	$(1/\sqrt{3})a$	0	$+uc$	
	F_3	$(1/\sqrt{3})a$	0	$(1/2 + u)c$	
	F_4	$(1/2\sqrt{3})a$	$-1/2a$	$(1/2 - u)c$	
ABCABC	C_1	0	0	$-zc$	$a = 2.5406$; $c = 14.2430$;
(hexagonal)	C_2	$(1\sqrt{3})a$	0	$+zc$	$z = 0.014063$;
	C_3	$(1\sqrt{3})a$	0	$(1/3 - z)c$	$u = 0.11913$;
	C_4	$(1/2\sqrt{3})a$	$-1/2a$	$(1/3 + z)c$	
	C_5	0	0	$(2/3 + z)c$	
	C_6	$(1/2\sqrt{3})a$	$-1/2a$	$(2/3 - z)c$	
	F_1	0	0	$-uc$	
	F_2	$(1/\sqrt{3})a$	0	$+uc$	
	F_3	$(1/\sqrt{3})a$	0	$(1/3 - u)c$	
	F_4	$(1/2\sqrt{3})a$	$-1/2a$	$(1/3 + u)c$	
	F_5	0	0	$(2/3 + u)c$	
	F_6	$(1/2\sqrt{3})a$	$-1/2a$	$(2/3 - u)c$	
AA′/A′A	C_1	0	0	$-zc$	$a = 2.5445$; $c = 9.4871$;
(hexagonal)	C_2	$(1/\sqrt{3})a$	0	$+zc$	$z = 0.021433$;
	C_3	$(1/\sqrt{3})a$	0	$(1/2 - z)c$	$u = 0.17748$;
	C_4	0	0	$(1/2 + z)c$	
	F_1	0	0	$-uc$	
	F_2	$(1/\sqrt{3})a$	0	$+uc$	
	F_3	$(1/\sqrt{3})a$	0	$(1/2 - u)c$	
	F_4	0	0	$(1/2 + u)c$	
AB/B′A′	C_1	0	0	$-zc$	$a = 2.5401$; $c = 18.995$;
(hexagonal)	C_2	$(1/\sqrt{3})a$	0	$+zc$	$z = 0.01147$; $u = 0.08815$;
	C_3	0	0	$(1/4 - z)c$	
	C_4	$(1/2\sqrt{3})a$	$-1/2a$	$(1/4 + z)c$	
	C_5	$(1/2\sqrt{3})a$	$-1/2a$	$(1/2 - z)c$	
	C_6	0	0	$(1/2 + z)c$	
	C_7	$(1/\sqrt{3})a$	0	$(3/4 - z)c$	
	C_8	0	0	$(3/4 + z)c$	
	F_1	0	0	$-uc$	
	F_2	$(1/\sqrt{3})a$	0	$+uc$	
	F_3	0	0	$(1/4 - u)c$	
	F_4	$(1/2\sqrt{3})a$	$-1/2a$	$(1/4 + u)c$	
	F_5	$(1/2\sqrt{3})a$	$-1/2a$	$(1/2 - u)c$	
	F_6	$(1/2\sqrt{3})a$	$-1/2a$	$(2/3 - u)c$	
	F_7	$(1/\sqrt{3})a$	0	$(3/4 - u)c$	
	F_8	0	0	$(3/4 + u)c$	

TABLE 2
Relative Energies per C–F Unit for Various Stacking Sequences of Graphite Monofluoride

Sequence	ΔE/per C–F unit [eV][a]	Band gap [eV]	Number of atoms in the cluster
AAA (boat conformation)	1.67	6.51	23 400
AAA (chair conformation)	0.69	6.55	43 740
ABAB (chair conformation)	0.68	6.47	27 000
ABCABC (chair conformation)	0.00	—	40 500
AA′/A′A (chair conformation)	0.01	—	27 000
AB/B′A′ (chair conformation)	0.43	5.84	38 148

[a] Relative energies are presented with respect to the most stable *ABCABC* conformation.

-0.14) show only a small polar character of these bonds. The optimized C–C bonds in neighboring carbon atoms are in the $1.53 \rightarrow 1.58 \times 10^{-10}$ m range. From these results it may be concluded that the properties of individual C–C and C–F bonds are in the range of analogous bonds in saturated fluorinated hydrocarbons.

The optimized structures for all possible stacking sequences (see Table 1) were used for band structure calculations of graphite monofluoride. The results of the calculations are presented in Fig. 3. It is seen that three types of sequences (*AAA*, *ABAB*, and *AB′/B′A′* sequences) have insulating properties, while the other two (*AA′/A/A* and *ABCABC* sequences) are of semimetallic character. This follows from the overlap between valence and conductive bands. The latter result explains the weak conductive properties of real graphite monofluoride (34–37).

More on the nature of valence and conductive bands can be seen from Fig. 4, where projected density of states in the vicinity of the Fermi level is plotted. For this figure we have chosen one of the insulating systems (*AAA* sequence) and compared it with two conductors (*AB/B′A′* and *ABCABC* sequences).

The p_x and p_y orbitals of carbon and p_z orbitals of fluorine are dominant at the top of the valence bands for the insulator. In this case, the nonzero densities of the valence and conductive bands are far from the Fermi level.

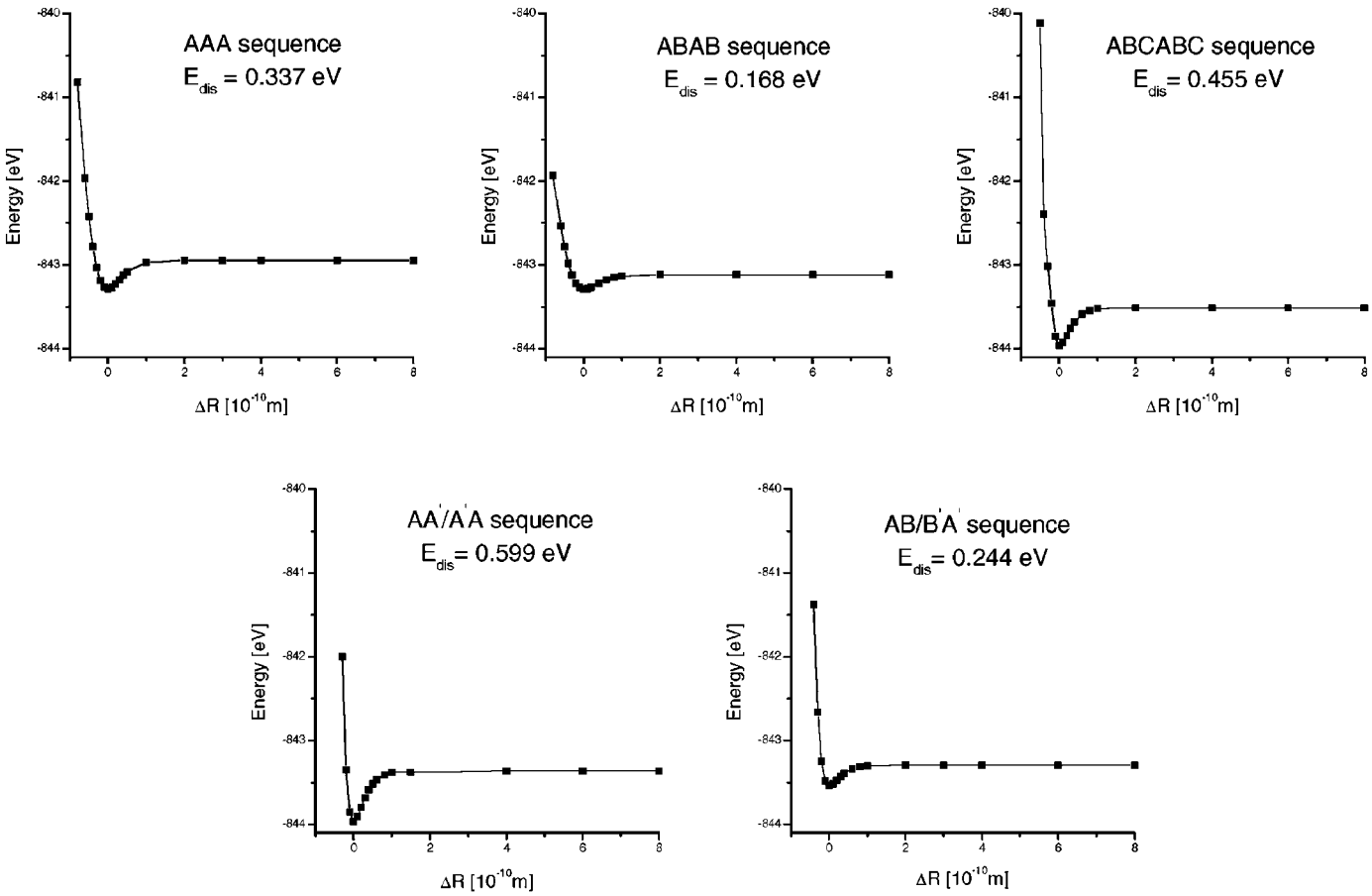

FIG. 2. Interlayer dissociation curves for various stacking sequences of graphite monofluoride.

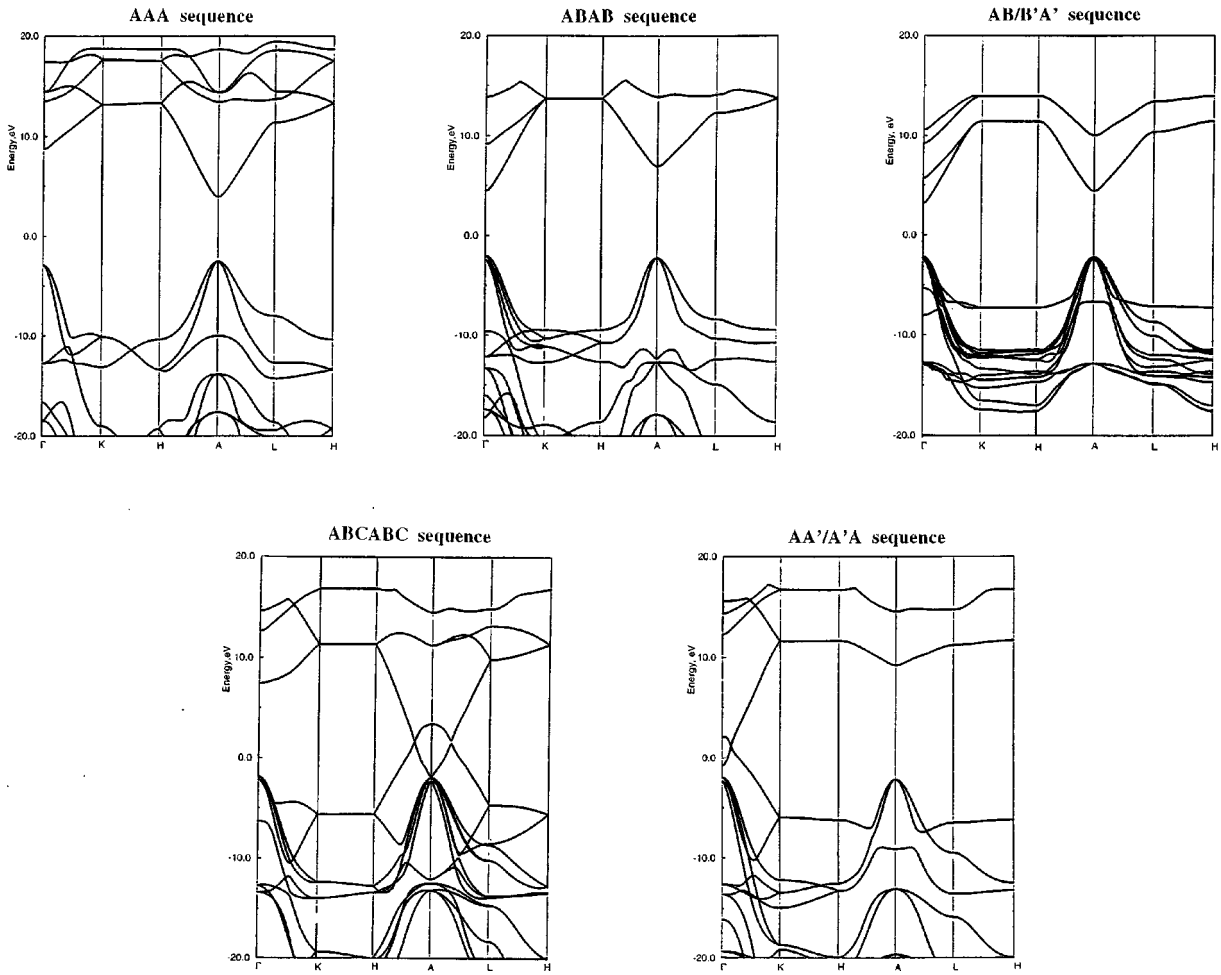

FIG. 3. Energy band structure along the main symmetry directions of the first Brillouin zone for various stacking sequences of graphite monofluoride.

For conductive sequences, the dominating contribution to the valence band around the Fermi level are due to p_z orbitals (perpendicular to the hexagonal layers) on the carbon and also fluorine atoms. It is clearly seen that the density of states for p_z orbitals continuously passes through the Fermi level, hence, conductive bands can be easily populated as a result of weak external potentials or for temperatures higher than 0 K.

The semimetallic character disappeared altogether when a single layer was considered. In this case, the gap between the valence and conductive bands was about 8 eV, which is even higher than for all three-dimensional structures. This, undoubtedly, confirms that interlayer interactions are responsible for the conductive properties of the *ABCABC* and $AA'/A'A$ configurations of graphite monofluoride.

CONCLUSIONS

The results of the calculations of geometric and electronic properties of the graphite monofluoride can be summarized as follows:

- Intercalated fluorine atoms form strong covalent and weakly polarized bonds with carbon atoms in the single layer, as expected.
- The chair conformation of individual layers is more stable as compared to the boat conformation of C_6 hexagon rings. The transition between these two conformations is symmetry forbidden reaction.
- Various stacking sequences of graphite monofluoride are very close on the energy scale, which suggests that in the real structure of graphite monofluoride, statistical distribution of various types of sequences can occur. In such a type of arrangement the maximal entropy contribution leads to the minimum of the Gibbs energy.
- Interlayer bond energies are very small, which corresponds to excellent lubricant properties of this type of material.
- The band structure calculations showed that the layered graphite monofluoride has insulating properties for some of the stacking sequences, while other stacking sequences have a semimetallic character. These results explain weak overall conductive properties of the real graphite monofluoride.

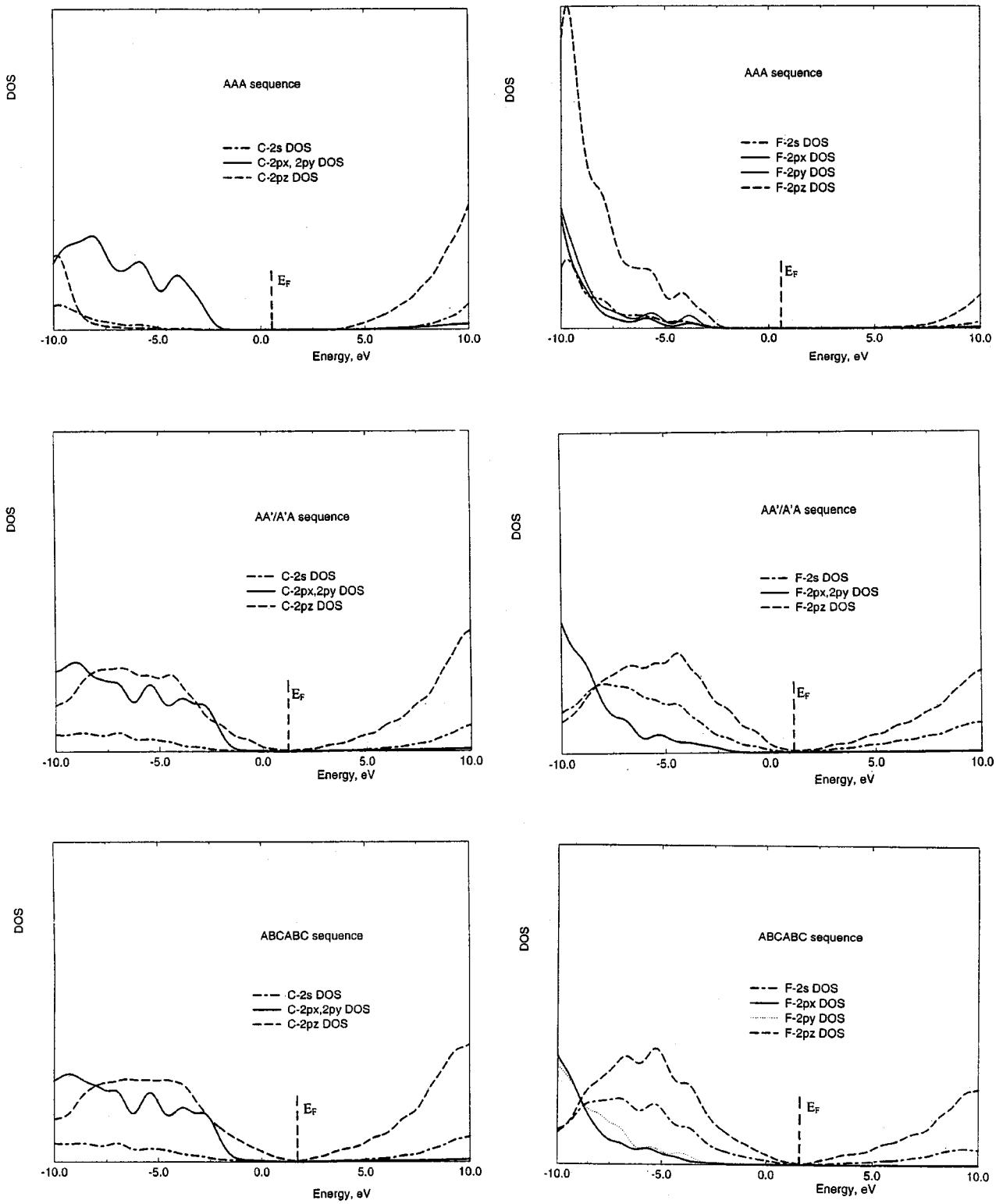

FIG. 4. Density of states around the Fermi level for nonconductive (*AAA*) and conductive (*AA′/A′A* and *ABCABC*) type of sequences.

ACKNOWLEDGMENTS

The authors express cordial thanks to S-Tech, Inc., and Supercomputing Centre, Brno, for the arrangement of computational facilities and Slovak Grant Agency VEGA for partial financial support (Contracts A-13/99 and 1/4012/97).

REFERENCES

1. O. Ruff, O. Bretschneider, and F. Elert, *Z. Anorg. Allg. Chem.* **217,** 1 (1934).
2. W. Rüdorff and G. Rüdorff, *Z. Anorg. Allg. Chem.* **253,** 281 (1947).
3. W. Rüdorff and K. Brodensen, *Z. Naturforch. B* **12,** 595 (1957).
4. W. Rüdorff, *Adv. Inorg. Chem. Radiochem.* **1,** 230 (1959).
5. L.B. Ebert, *Ann. Rev. Mater. Sci.* **6,** 181 (1976).
6. J.-C. Charlier, X. Gonze, and J.-P.Michenaud, *Phys. Rev. B* **43,** 4579 (1991).
7. J. L. Wood, R. B. Badachhape, R. J. Lagow and J. L. Margrave, *J. Phys. Chem.* **73,** 3139 (1969).
8. N. Watanabe, and M. Takashima, "On the Formation of Graphite Fluoride." Kyoto University Press, Kyoto, 1973.
9. T. Nakajima and N. Watanabe, "Graphite Fluorides and Carbon–Fluorine Compounds." CRC, Boca Raton, FL, 1974.
10. R. L. Fusaro and H. E. Sliney, *A.S.L.E. Trans.* **13,** 56 (1970).
11. R. L. Fusaro and H. E. Sliney, *A.S.L.E. Trans.* **16,** 189 (1973).
12. H. Glisser, M. Petronio, and H. Shapiro, *J. Am. Lubr. Eng.* **28,** 161 (1972).
13. P. Sutor, *Mater. Res. Bull.* **XVI** (5), 24, (1991).
14. N. Watanabe and M. Ishii, *Denki Kagaku* **29,** 364 (1961).
15. N. Watanabe, M. Inoue, and S. Yoshizawa, *Denki Kagaku* **31,** 693 (1963).
16. N. Watanabe, H. Takenaka, and M. Takashima, *Nippon Kagaku Kaishi* **1973,** 487.
17. N. Watanabe, M. Takashima, and K. Takahashi, *Nippon Kagaku Kaishi*, **1974,** 1033.
18. R. Kamarchik and J. L. Margrave, *Acc. Chem. Res.* **11,** 296 (1978).
19. J. Mahajam, R. B. Badachhape, and J. L. Margrave, *Inorg. Nucl. Chem.* Lett. **10,** 1103 (1974).
20. N. A. W. Holzwarth, S. Q. Louie, and S. Rabii, *in* "Intercalated Graphite" (M. S. Dresselhaus, G. Dresselhaus, J. E. Fisher, and M. J. Moran, Eds.), MRS Symposia Proceedings, No. 20. North Holland, New York, 1982.
21. R. Yazami and A. Hamwi, *Solid State Ionics* **28–30,** 1756 (1988).
22. D. E. Parry, J. M. Thomas, B. Bach, and E. L. Evans, *Chem. Phys. Lett.* **29,** 128(1974).
23. H. Touhara, K. Kadono, Y. Fujii, and N. Watanabe, *Z. Anorg. Allg. Chem.* **544,** 7 (1987).
24. L. B. Ebert, Ph.D. thesis. Stanford University, 1975.
25. L. B. Ebert, J. I. Brauman, and R. A. Huggins, *J. Am. Chem. Soc.* **96,** 7841 (1974).
26. J. Noga, P. Baňacký, S. Biskupič, R. Boča, P. Pelikán, M. Svrček, and A. Zajac, *J. Comput. Chem.* **20,** 253 (1999).
27. A. Zajac, P. Pelikán, J. Noga, P. Baňačký, S. Biskupič, and M. Svrček, *J. Phys. Chem. B*, in press.
28. J. A. Pople and D. L. Beveridge, "Approximate Molecular Orbital Theory," McGraw–Hill, New York, 1970.
29. R. Boča, *Int. J. Quantum Chem.* **31,** 941 (1987).
30. R. Boča, *Int. J. Quantum Chem.* **34,** 385 (1988).
31. W. H. Press, S. A. Teukolsky, W. T. Vetterling, and B. B. Flammery, "Numerical Recipes in Fortran." Cambridge University Press, Cambridge, UK, 1992.
32. V. Kvasnicka and J. Pospíchal, *Chem. Intell. Lab. Syst.* **39,** 161 (1997).
33. J. Noga, P. Baňacký, S. Biskupič, P. Pelikán, and A. Zajac, "SOLID98, A Program System for Calculating Electronic Structure of Periodic Solid State Systems." S-Tech, Inc., Bratislava, 1998. [http://www.stech.sk.]
34. I. Ohana, *Phys. Rev. B* **39,** 1914 (1989).
35. T. Nakajima, M. Kawaguchi, and N. Watanabe, *Synth. Metals* **7,** 117 (1983).
36. T. Nakajima, N. Watanabe, I. Kameda, and M. Endo, *Carbon* **24,** 343 (1986).
37. T. Nakajima, M. Kawaguchi, and N. Watanabe, *Solid State Ionics* **11,** 55 (1983).